Radiation Measurements 67 (2014) 67–76

Contents lists available at ScienceDirect

Radiation Measurements

journal homepage: www.elsevier.com/locate/radmeas

Monte Carlo simulations of luminescence processes under quasi-equilibrium (QE) conditions

Vasilis Pagonis*, Ethan Gochnour, Michael Hennessey, Charles Knower

Physics Department, McDaniel College, Westminster, MD 21157, USA

HIGHLIGHTS

- A simplified Monte Carlo method for TL and OSL is presented.
- Method is based on General One Trap model, and quasi-equilibrium conditions.
- Small clusters of a few traps can lead to multiple peaks in TL and LM-OSL signals.
- Effects of retrapping and degree of trap filling are simulated.

ARTICLE INFO

Article history:
Received 11 April 2014
Received in revised form
30 May 2014
Accepted 12 June 2014
Available online 20 June 2014

Keywords:
Thermoluminescence
LM-OSL
Monte Carlo simulations
GOT kinetic model

ABSTRACT

Previous researchers have carried out Monte Carlo simulations of thermoluminescence (TL) phenomena by considering the allowed transitions of charge carriers between the conduction band, electron traps and recombination centers. Such simulations have demonstrated successfully the effect of trap clustering on the kinetics of charge carriers in a solid, and showed that trap clustering can significantly change the observed luminescence properties. While such Monte Carlo simulations have been carried out for TL, there has been no such trap clustering studies for optically stimulated luminescence phenomena (OSL). This paper presents a simplified method of carrying out Monte Carlo simulations for TL and linearly modulated optically stimulated luminescence (LM-OSL) phenomena, based on the General One Trap (GOT) model, which is a special case of the one trap one recombination center model (OTOR) when quasi-equilibrium conditions (QE) hold. The simulated results show that the presence of small clusters consisting of a few traps in a solid can lead to multiple peaks in both the TL and LM-OSL signals. The effects of retrapping and degree of trap filling are simulated for such multi-peak luminescence signals, and insight is obtained into the mechanism producing these peaks. The method presented in this paper can be easily generalized for other types of luminescence solids in which the recombination probability varies with time.

1. Introduction

Recently luminescent materials consisting of nanoclusters with only a few atoms have attracted significant attention. The synthesis and characterization of such nanodosimetric materials has become an increasingly active research area, and it has been shown that their physical properties can be different from those of similar conventional microcrystalline phosphors (see for example Salah, 2011; Sun and Sakka, 2014; Eliyahu et al., 2014; and references therein). It has been suggested that traditional energy band models may not be applicable for some of these nanodosimetric materials, because of the existence of strong spatial correlations between traps and recombination centers. Such spatially correlated systems are also likely to be found in polycrystalline and low-dimensional structures, as well as in materials which underwent high energy/high dose irradiations which create groups of large defects. The luminescence properties of such spatially correlated materials can be simulated by using Monte Carlo techniques.

Monte-Carlo methods for the study of thermoluminescence (TL) were presented in the papers by Mandowski (2001, 2006; 2008) and Mandowski and Świątek (1992, 1996; 2000). These authors suggested that usually the number of carriers in a sample is large and the differential equations used in traditional kinetic models describe the system properly. However, in some solids one must

* Corresponding author. Tel.: +1 410 857 2481; fax: +1 410 386 4624.
E-mail address: vpagonis@mcdaniel.edu (V. Pagonis).

http://dx.doi.org/10.1016/j.radmeas.2014.06.005
1350-4487/

consider clusters of traps as separate systems, since the continuous differential equations are not valid. Kulkarni (1994) described how the Monte Carlo technique can be used to simulate TL and thermally stimulated conductivity (TSC) phenomena, with emphasis on the required calculation time, statistical errors and comparison with other methods.

Typically the Monte Carlo calculations are performed with the total population of carriers simultaneously, and in each step of the Monte-Carlo simulation one finds the lowest transition time for all possible transitions, and this is the only transition which is executed. Mandowski and Świątek (1996) simulated TL spectra for different trap parameters and different correlations between traps and recombination centers, and compared the resulting TL glow curves with the empirical general order model. For relatively small trap clusters large differences were found between the modeled TL/TSC curves and the empirical general order kinetics expressions. These authors showed conclusively that spatially correlated effects become prominent for low concentrations of thermally disconnected traps and for high recombination situations. Additional applications of Monte Carlo simulations in luminescence were presented by Mandowski et al. (2010) for determining the thermal-quenching function, by Bailey (2004) on an empirical energy band model for quartz and by Thompson (2007) on the SAR protocol in quartz. In two additional Monte Carlo applications in luminescence Pagonis and Kitis (2012) studied several popular luminescence models using random combinations of variables, while Pagonis et al. (2011) applied the same technique in simulating several dating protocols for quartz. Adamiec et al. (2004, 2006) used a method of random variation of kinetic parameters to develop a genetic algorithm for luminescence models. Rodríguez-Villafuerte (1999) used a Monte Carlo approach in their application of the track-interaction model on the supralinearity in the TL response.

The above mentioned studies have focused on the properties of TL glow curves using Monte Carlo simulations. To the best of our knowledge, there have been no attempts to simulate the effect of trap clusters on the properties of optically stimulated luminescence (OSL) signals.

The goals of this paper are:

1. To carry out Monte Carlo simulations of trap clustering phenomena, by using a simple technique based on the general one trap (GOT) model of luminescence.
2. To show that this simple technique can also be used for simulating OSL phenomena.
3. To obtain physical insight into the nature of the simulated multi-peak TL and linearly modulated OSL signals (LM-OSL), by varying the parameters in the model.

2. The GOT model

Previous Monte Carlo work on TL signals has been carried out within the framework of the one-trap one-recombination center (OTOR) model of luminescence. The Monte Carlo simulation technique used in this paper is based on the GOT model, which can be derived from the OTOR model using the quasistatic equilibrium conditions (QE). For an overview of previous work using the GOT and OTOR models, the reader is referred to the relevant books (see for example Chen and Pagonis, 2011; Pagonis et al., 2006). In this section the main equations of the OTOR and GOT models are summarized.

The rate equations of the OTOR model for TL are:

$$\frac{dn}{dt} = -ns\exp\left(-\frac{E}{kT}\right) + n_c(N-n)A_n, \tag{1}$$

$$\frac{dn_c}{dt} = -\frac{dn}{dt} - n_c m A_m. \tag{2}$$

The time-dependent TL intensity is given by

$$I_{TL}(t) = -\frac{dm}{dt} = n_c m A_m. \tag{3}$$

In the above equations N (cm^{-3}) is the total concentration of dosimetric traps, n (cm^{-3}) is the concentration of filled dosimetric traps, n_c (cm^{-3}) is the instantaneous concentration of electrons in the conduction band. E (eV) and s (s^{-1}) represent the thermal activation energy and the frequency factor of the dosimetric trap, correspondingly. The concentration m (cm^{-3}) of the recombination centers (RC) at all times is given by $m = n + n_c$, so that charge balance is maintained in the system. A_n and A_m (cm^3s^{-1}) are the capture coefficients of the trap and recombination center respectively, T the absolute temperature and k the Boltzmann constant. The initial concentrations of filled traps at time $t = 0$ are denoted by the symbol n_0, and a linear heating rate β is assumed during the heating experiment.

The quasi–static equilibrium (QE) condition is commonly used as a simplifying assumption in luminescence modeling and is expressed by the relations (Chen and Pagonis, 2013):

$$\left|\frac{dn_c}{dt}\right| \langle\langle \left|\frac{dn}{dt}\right|, \left|\frac{dm}{dt}\right| \quad \text{and} \quad n_c \langle\langle n, \quad n \simeq m \tag{4}$$

By applying these QE conditions to the system of differential equations (1)–(3), one obtains the general one trap equation (GOT) for TL intensity:

$$I_{TL}(t) = -\frac{dn}{dt} = \frac{A_m n^2 s \exp\left(-\frac{E}{kT}\right)}{(N-n)A_n + nA_m}. \tag{5}$$

In the case of continuous-wave OSL signals (CW-OSL), one replaces the rate of thermal excitation $p = sexp(-E/kT)$ in equation (1), with the corresponding constant rate λ (s^{-1}) for optical excitation processes and equation (5) becomes:

$$I_{CW-OSL}(t) = -\frac{dn}{dt} = \frac{A_m \lambda n^2}{(N-n)A_n + nA_m} \tag{6}$$

In the special case of LM-OSL experiments, one uses a rate of optical excitation $\lambda = bt$ which increases linearly with time, where b is a parameter which depends on the experimental conditions and on the optical cross section for the traps under consideration, and t is the time elapsed from the start of the LM-OSL experiment. In this LM-OSL case equation (6) becomes:

$$I_{LM-OSL}(t) = -\frac{dn}{dt} = \frac{A_m b n^2 t}{(N-n)A_n + nA_m} \tag{7}$$

Equations (5) and (7) cannot be solved analytically; however they can be solved numerically using standard commercial software packages.

3. The "brute force" Monte Carlo method based on equations (5) and (7)

The basic Monte Carlo technique using differential equations like equation (5) or (7) is found in many standard textbooks of simulations in Statistical Physics (see for example Gould and Tobochnik, 1995; Landau and Binder, 2013; and references therein). The prototype application of these so-called "brute force" Monte Carlo methods is radioactive decay, in which one assumes

that all radioactive nuclei are identical, and that during any time interval Δt each nucleus has the same decay probability λ (s^{-1}) per unit time. The dimensionless probability P for the nucleus decaying within a time interval Δt is $P = \lambda \Delta t$, and one chooses a suitable value of Δt so that $P<<1$. In this simple algorithm one chooses a nucleus and a random number r uniformly distributed in the unit interval $0 \leq r < 1$ is generated. If $r \leq P$ the nucleus decays, otherwise it does not; all non-decayed remaining nuclei are tested during each time interval Δt, and several decay events can take place during each time interval Δt. The value of the remaining nuclei n *is* updated at the end of each time interval Δt, and the process is continued until there are no nuclei left. The well-known differential equation for this radioactivity process is $dn/dt = -\lambda n$, where n represents a continuous variable. In the case of the Monte Carlo simulations this differential equation becomes a *difference* equation $\Delta n = -\lambda n \Delta t$ for the discrete variable n.

The method used in this paper is completely analogous to this Monte Carlo technique for radioactive decay. A fixed time interval $\Delta t = 1$ s was used in all simulations presented in this paper, and equations (5) and (7) become difference equations for TL and LM-OSL:

$$\Delta n = \frac{n^2 s \exp\left(-\frac{E}{kT}\right)}{(N-n)r + n}\Delta t, \tag{8}$$

$$\Delta n = \frac{bn^2 t}{(N-n)r + n}\Delta t, \tag{9}$$

where the substitution $r = A_n/A_m$ was made for the retrapping ratio. Equations (8) and (9) are the difference equations forming the basis of the simulations described in the rest of this paper. The corresponding TL and LM-OSL intensities $I_{TL}(T)$ and $I_{LM-OSL}(t)$ are calculated from the values of Δn in equations (8) and (9) using the expressions:

$$I_{TL}(T) = -\frac{1}{\beta}\frac{\Delta n}{\Delta t}, \tag{10}$$

and

$$I_{LM-OSL}(t) = -\frac{\Delta n}{\Delta t}. \tag{11}$$

It is important to note that equations 8–11 are difference equations for the integer variable n, while the original equations (1)–(3) in the OTOR model represent differential equations for continuous variables.

For the system of trap clusters described in this paper, one must make a clear distinction between local variables describing the internal structure of each cluster, and global variables which describe the whole group of clusters. These local and global variables are described next, and are also listed in Table 1 for easy reference. Typical values of these parameters are also shown in Table 1.

The system simulated in this paper has some similarities to the one used by Mandowski and Świątek (1996), and consists of a large number of small clusters of traps and recombination centers. The local physical parameters characterizing each cluster are: the total number of traps per cluster N_{traps}, the number of initially filled traps per cluster n_{filled} (in general $n_{filled} \leq N_{traps}$), and the instantaneous number of remaining filled traps in the cluster denoted by n_{local}. As the system develops in time during the optical or thermal stimulation process, the value of the local variable n_{local} will decrease from its initial value of n_{filled} to zero, as more recombinations take place within the cluster.

Table 1
Listing of local and global variables used in the simulations of this paper, and their typical values (see also Fig. 1 for a pictorial presentation of the local variables).

	Description	Typical value
Local variables		
n_{local}	The instantaneous (time dependent) number of remaining filled traps in the cluster.	n_{local} = variable = 3-0
n_{filled}	The number of initially filled traps per cluster n_{filled} In general $n_{filled} \leq N_{traps}$.	$n_{filled} = 3$
N_{traps}	The total number of traps per cluster	$N_{traps} = 4$
Global variables		
n	The total instantaneous (time dependent) number of remaining filled traps in the system. This is calculated by summing over all clusters $n = \sum_{all\ clusters} n_{local}$.	n = variable = 3×10^5
n_o	The total number of initially filled traps in the system. n_o is found from $n_o = N_{clusters} n_{filled}$ (with $n_o \leq N$).	$n_o = 3\times10^5$
$N_{clusters}$	The number of trap clusters in the system.	$N_{clusters} = 10^5$

In terms of global variables, the system is described by the number of trap clusters in the system $N_{clusters}$. The total number of available traps in the system is given by the product $N = N_{clusters} N_{traps}$, while the total number of initially filled traps n_o is given by $n_o = N_{clusters} n_{filled}$ (with $n_o \leq N$). The equalities $n_{filled} = N_{traps}$ and $n_o = N$ denote a system with all traps initially filled. The total instantaneous number of filled traps is denoted by the global variable n, and is calculated as the sum of the locally remaining filled traps n_{local} over all clusters in the system, i.e. $n = \sum_{all\ clusters} n_{local}$.

Clearly the variables n_{local}, n_{filled} and N_{traps} represent local variables characterizing each cluster in the system, while the global variables $N_{clusters}$, n_o, n and N characterize the whole system of trap clusters.

Fig. 1 shows schematically an example of such a system of small trap clusters, in which there are 4 traps in each cluster ($N_{traps}=4$ shown as both open and solid circles), with only 3 of them being initially filled ($n_{filled}=3$ shown as solid circles). One ensures the charge balance in the system, by assuming the existence of an equal number of 4 luminescence centers (shown as both open and solid stars), 3 of which have been activated (shown as solid stars). In this example one could simulate, for instance, a large number of clusters $N_{clusters}=10^5$ in the system, resulting in a total number of $n_o = N_{clusters} n_{filled} = 3x10^5$ initially filled traps. From a physical point of view, the activated luminescence centers may exist in physical proximity to the filled traps, since they both could have been

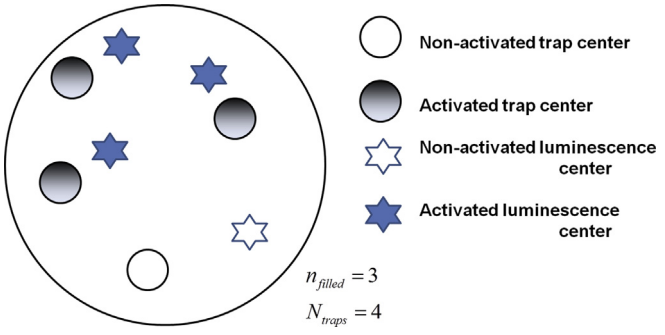

Fig. 1. Schematic representation of a small trap cluster, consisting of a total of four traps in each cluster ($N_{traps} = 4$ shown as both open and solid circles). Only 3 of these traps are initially filled. ($n_{filled} = 3$ shown as solid circles). Charge balance in the system is ensured by assuming the existence of an equal number of 4 luminescence centers (shown as both open and solid stars), 3 of which have been activated (shown as solid stars). The solid is assumed to consist of a large number of clusters (e.g. $N_{clusters} = 10^5$).

created simultaneously during the irradiation process. As the system of trap clusters in Fig. 1 develops in time, the local variable n_{local} will vary from an initial value of n_{local}=n_{filled}=3 to its final value of n_{local}=0 at the end of the thermal/optical excitation process. Similarly the global variable n will vary from an initial value of n_o=3x10^5 to its final value of n=0 at the end of the thermal/optical excitation process.

By using the local variables n_{local} andN_{traps} to replace the variables n and N, equations (8)–(9) become:

$$\Delta n_{local} = \frac{n_{local}^2 s \exp\left(-\frac{E}{kT}\right)}{(N_{traps} - n_{local})r + n_{local}} \Delta t, \tag{12}$$

$$\Delta n_{local} = \frac{b n_{local}^2 t}{(N - n_{local})r + n_{local}} \Delta t. \tag{13}$$

The luminescence intensity from the overall system of trap clusters will consist of the sum of expressions (10) and (11) over all clusters in the system, i.e.:

$$I_{TL}(T) = \sum_{all\ clusters} \left(-\frac{1}{\beta} \frac{\Delta n_{local}}{\Delta t} \right), \tag{14}$$

and

$$I_{LM-OSL}(t) = \sum_{all\ clusters} \left(-\frac{\Delta n_{local}}{\Delta t} \right). \tag{15}$$

The physical implications of using the local variables n_{local} and N_{traps} in equations 12–15 are considered in more detail in the Discussion section of this paper.

In practical terms, software implementation of equations 12–15 for the system of trap clusters shown in Fig. 1 proceeds as follows. At time $t = 0$ the initial values are n_{local}=n_{filled}=3 and the evolution of the system is followed during an appropriate time interval Δt. The probability P for an electron in a single cluster to recombine radiatively within the time interval Δt is given by the fractional expression multiplying Δt in the right hand side of equations (12) and (13). As in the case of the previously mentioned radioactivity example, one chooses a suitable value of Δt so that P<<1, and a random number r uniformly distributed in the unit interval $0 \leq r < 1$ is generated. If $r \leq P$ the electron recombines radiatively, otherwise it does not; all non-recombined remaining electrons in the cluster are tested during each time interval Δt, and several recombination events could take place during each time interval Δt. The value of the remaining electrons n_{local} in the cluster is updated at the end of each time interval Δt, and the process is continued until there are no electrons left in the cluster (i.e. until n_{local}=0). This process is repeated for the large number of clusters $N_{clusters}$=10^5 in the system, resulting in the total luminescence intensity given by equations (14) and (15). The effect of using different values of Δt was tested by repeating the simulations using Δt = 0.1, 0.01, 1 s; the simulation results stayed unaffected by changing the value of Δt within this range of values.

The simulations in this paper were carried out using the commercial software package *Mathematica*. A double iterative loop is used as described in the previous paragraph, with the inner loop simulating a single cluster using local variables, and with the outer loop simulating the whole group of clusters using global variables. A third iterative loop advances the time t by increments of Δt, simulating the thermal/optical stimulation of the system. Typical running times for $N_{clusters}$=10^5 clusters in the system is ~1–5 min, and the simulations use the random number generator embedded in *Mathematica*. No special packages or libraries are required for the straightforward simulations presented in this paper.

The implicit physical assumption in this description of the system is that each cluster acts as an independent entity as far as the luminescence process is concerned, since each electron participates only in local processes within the cluster. This implicit assumption and its possible physical consequences are examined further in the Discussion section of this paper.

4. Simulation results

In this section the effect of trap clustering on the TL and LM-OSL signals is simulated, under the assumption that QE conditions hold during the luminescence process.

4.1. Simulation of TL and LM-OSL signals for large trap clusters

Fig. 2 shows the results of a Monte Carlo simulation for the TL signal using equation (12). The kinetic parameters used in these simulations are $s = 10^{10}$ s^{-1}, $E = 0.9$ eV, a linear heating rate β=1 K/s and the retrapping ratio $r = A_n/A_m = 10$. The example in Fig. 2 shows the simulation of a system with rather large clusters, each cluster consisting of 100 initially completely filled traps, i.e. n_{filled}=N_{traps}=100. The system consists of 100 such clusters.

($N_{clusters}$=100), resulting in a total number of n_o=$N_{clusters}n_{filled}$=10^4 initially filled traps.

Fig. 2a shows the number of remaining filled traps $n(T)$ as a function of the temperature T, while Fig. 2b shows the corresponding TL signal, obtained by using the difference equation (14). Inspection of Fig. 2ab shows that the statistical fluctuations in the number of remaining trapped carriers $n(T)$ in Fig. 2a, are much smaller than the corresponding fluctuations in the TL signal shown in Fig. 2b. This is due to the fact that $n(T)$ is calculated directly from equation (12), while the TL signal is calculated from the differences $\Delta n/\Delta T$ between successive values of $n(T)$, according to equation (14). Consecutive stochastic fluctuations in the values of $n(T)$ will propagate in the values of TL in equation (14), resulting in larger scattering of the TL values in Fig. 2b at any temperature T.

There are two standard methods by which the stochastic fluctuations shown in Fig. 2b can be reduced. In accordance with standard Monte Carlo practices, one can repeat the simulations in Fig. 2ab several times by using a different set of random numbers each time and averaging the results, leading to smaller statistical fluctuations. In the second method the statistical error in $n(T)$ and in $\Delta n/\Delta T$ can be decreased by increasing the total number of charge carriers tracked in the system. As discussed in some detail by Kulkarni (1994), the statistical error in the simulation of Fig. 2b depends on the temperature T along the TL glow curve, on the temperature interval ΔT and on the total number of carriers being tracked, N_{total}. The Monte Carlo statistical error is expected to be inversely proportional to the square root N_{total}.

Fig. 2c shows the results of repeating the simulation of Fig. 2b by varying the total number of initially filled traps in the system in the range N_{total}=n_o=100–10^6, while the rest of the parameters in the model are kept fixed. Specifically Fig. 2c shows the statistical errors (standard deviation of the data) near the peak maximum at $T \simeq 150^oC$. These statistical errors are presented in Fig. 2c by the relative standard deviation of the simulated data σ_n/n and σ_{TL}/TL. The percent statistical error σ_{TL}/TL for the TL intensity (open circles in Fig. 2c) can be seen to decrease from ~100% for N_{total}=100 to about 10% for N_{total}=10^6. The corresponding statistical errors σ_n/n for the number of particles (solid circles in Fig. 2c) are almost an order of magnitude smaller. The log–log data in Fig. 2c has a negative linear slope of −0.48, confirming the expected $1/\sqrt{N_{total}}$ dependence of the statistical error in Monte Carlo simulations.

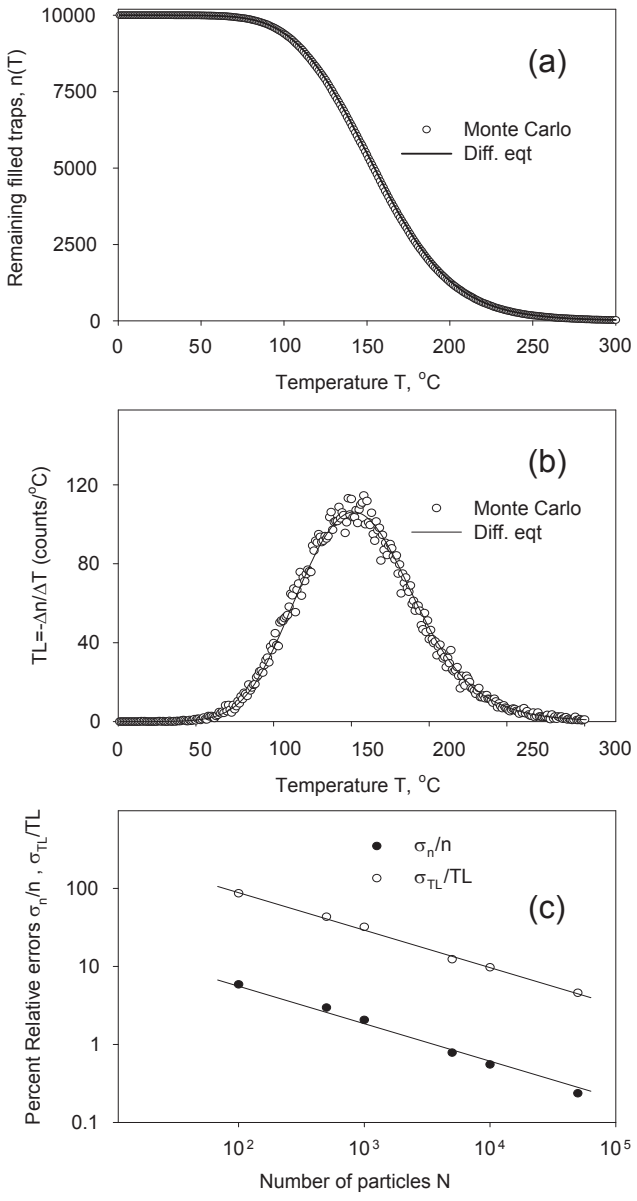

Fig. 2. Monte Carlo simulation for a TL experiment based on equation (8) for a system of $N_{clusters} = 100$ rather large clusters, each consisting of $N_{traps} = n_{filled} = 100$ initially filled traps per cluster. The parameters used are: $s = 10^{10}$ s^{-1}, $E = 0.9$ eV, β=1 *K/s*, $r = A_n/A_m = 10$, n_{filled}=N_{traps}=100, $N_{clusters}$=100, n_o=$N_{clusters}n_{filled}$=10^4. (a) Variation on the remaining number of trapped carriers $n(t)$ with the time *t*. (b) The TL signal corresponding to the simulation in (a), obtained by using the difference equation (10). (c) Percent statistical errors σ_n/n and σ_{TL}/TL of the simulated data at a temperature T~150 °C, obtained by repeating the simulation in (b) for N_{total}=100–10^6.

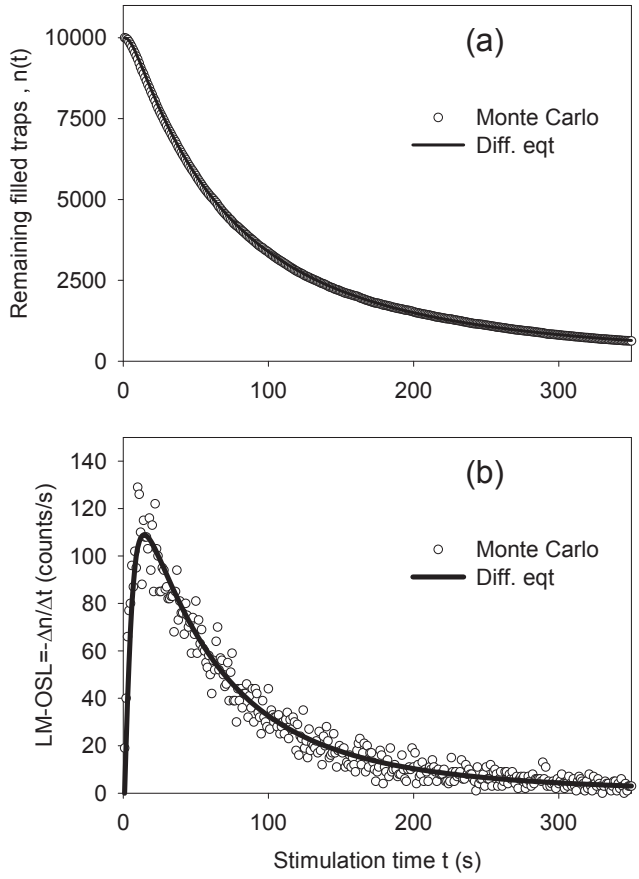

Fig. 3. Monte Carlo simulation for a LM-OSL experiment, based on equation (9). The parameters used are: $b = 0.002$ s^{-1}, $r = A_n/A_m = 10$, n_{filled}=N_{traps}=100,$N_{clusters}$=100, n_o=$N_{clusters}n_{filled}$=10^4. (a) Variation on the number of particles $n(t)$ with the optical stimulation time *t* and (b) The corresponding LM-OSL signal $I_{LM-OSL}(t)$=$-\Delta n/\Delta t$. The solid line in (a) and (b) represents the numerical solution of differential equation (7).

The solid line in Fig. 2a and b represents the numerical solution $n(T)$ and I_{TL}=$-1/\beta(dn/dT)$ of the differential equation (5), indicating that in the case of large clusters simulated in Fig. 2, the results of the Monte Carlo simulation approach the results from a uniform distribution of particles in the system (Mandowski and Świątek, 1998; and references therein).

Fig. 3 shows a similar Monte Carlo simulation for an LM-OSL experiment, based on equation (13). It is preferable to simulate LM-OSL experiments instead of CW-OSL, because the latter is a featureless signal that does not lend itself to easy visualization of the various components in the signal. The parameters used in the simulation of Fig. 3 are the same as in the TL simulation of Fig. 2, with the additional parameter in equation (13) being the optical stimulation parameter $b = 0.002$ s^{-1}. Fig. 3a shows the variation of the number of trapped electrons $n(t)$ as a function of the stimulation time *t*, while Fig. 3b shows the corresponding LM-OSL intensity $I_{LM-OSL}(t)$=$-\Delta n/\Delta t$. The solid lines in Fig. 3a and b represent the numerical solution of the differential equation (7). The agreement between the Monte Carlo simulation and the solution of the differential equation indicates the same behavior as in the case of Fig. 2, namely that in a system of large trap clusters the LM-OSL signals approaches the limit of a uniform distribution of particles.

The total area in the simulated data of Figs. 2b and 3b is equal to the total number of initially filled traps n_o=10^4. The simulations in Figs. 2 and 3 were repeated for larger values of n_o=10^5–10^6 and the results remained unchanged. It is also noted that the concept of clusters is not necessary for obtaining the results in Figs. 2 and 3. These figures are meant as a check of the effectiveness and self-consistency of the Monte Carlo method used in this paper, and they do not show cluster effects. In addition, the results in Figs. 2–3 are important because they show how the simulated results transition from the discrete-variable results of equations 12–15 to the continuous-variable results from the solution of the differential equations.

4.2. Simulations for clusters of different sizes: trap clustering effects

Fig. 4a shows the results of repeating the simulation of Fig. 2 for two different systems, in which the size of the clusters is changed,

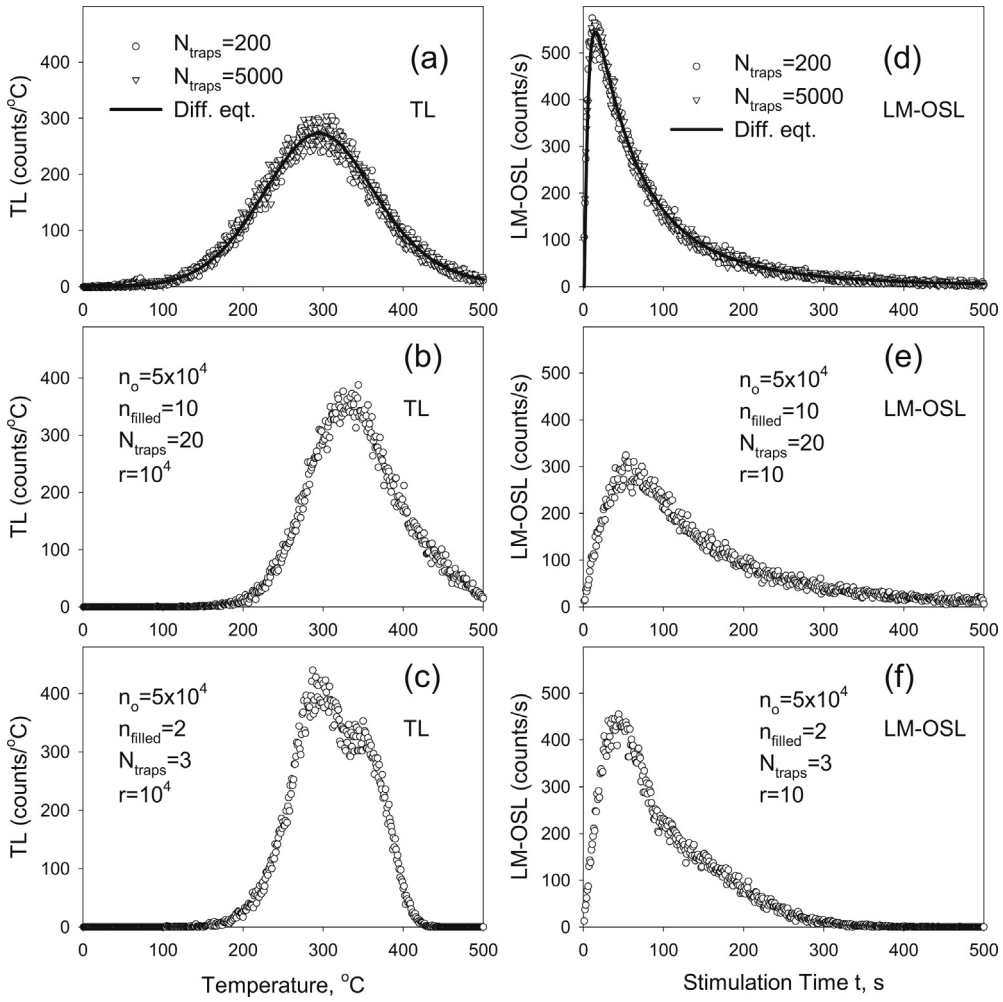

Fig. 4. (a) TL signal from two systems of very large size trap clusters The parameters are n_{filled}=N_{traps}=200, 5000, $s = 10^{10}$ s^{-1}, $E = 0.9$ eV, β=1 K/s, $r = A_n/A_m = 10^4$, n_o=5×10^4 .(b) TL signal from a system of medium size trap clusters. The parameters are the same as in (a) with n_{filled}=10 , N_{traps}=20. (c) TL signal from a system of very small trap clusters. The parameters are the same as in (a), with n_{filled}=2 , N_{traps}=3. (d) The same simulation as in Fig. 4a, for the case of LM-OSL signals. (e) The same simulation as in Fig. 4b, for the case of LM-OSL signals. (f) The same simulation as in Fig. 4c, for the case of LM-OSL signals. The parameters in Fig. 4d–f are $b = 0.002$ s^{-1} and $r = 10$.

while the total number of initially filled traps is kept the same. Specifically Fig. 4a shows the simulation of two large clusters with the corresponding total numbers of initially completely filled traps, n_{filled}=N_{traps}=200, 5000. The kinetic parameters used in these simulations are $s = 10^{10}$ s^{-1}, $E = 0.9$ eV, β=1 K/s and the retrapping ratio is large, $r = A_n/A_m = 10^4$. The total number of particles in the system is kept constant at n_o=$N_{clusters}N_{traps}$=5×10^4, while the size of the clusters is changed by varying the number of clusters $N_{clusters}$ in the system. Fig. 4a shows that the TL intensity from the two systems of different cluster sizes is the same, indicating that the luminescence signal from systems of large clusters is independent of the size of the cluster. The same results were obtained for even larger clusters with N_{traps}>5000, not shown here. Fig. 4d shows the same simulation as in Fig. 4a, for the case of LM-OSL signals. The optical stimulation parameter in Fig. 4d is $b = 0.002$ s^{-1} and the retrapping ratio is $r = 10$. These simulations in Fig. 4a and d support the conclusion that both the TL and LM-OSL signals from a system of large clusters withN_{traps}≥200 are independent of the size of the cluster, when the total number of particles in the system is kept constant.

The situation is seen to be different in Fig. 4b and c, which shows the same simulations as in Fig. 4a, repeated with clusters of smaller size, while the total number of initially filled traps is kept fixed at n_o=5×10^4. Specifically Fig. 4b shows the TL signal from a system of medium size trap clusters, in which each cluster consists of a total of 20 traps, ten of which are initially filled (n_{filled}=10 , N_{traps}=20). Fig. 4c shows TL from a system of very small size clusters, in which each cluster consists of a total of 3 traps, two of which are initially filled (n_{filled}=2 , N_{traps}=3). In all three examples in Fig. 4abc, the total number of initially filled traps is the same, n_o=5×10^4. The values of the rest of the parameters remain the same in Fig. 4abc. As the size of the clusters is decreased from Fig. 4a to c, the TL glow curves become narrower and a two-peak structure is seen clearly in Fig. 4c.

Similar examples for LM-OSL signals are shown in Fig. 4e and f, which shows the same simulations as in Fig. 4d, repeated for progressively smaller trap clusters. Fig. 4e shows a system of medium size trap clusters with n_{filled}=10 , N_{traps}=20. Fig. 4f shows a system of small size trap clusters with n_{filled}=2 , N_{traps}=3. In all three examples in Fig. 4def, the total number of initially filled traps is the same, n_o=5×10^4. The values of the rest of the parameters are the same in Fig. 4def.

The TL and LM-OSL signals in Fig. 4c and f shows clearly the presence of additional peaks, which have been attributed previously to trap clustering effects for the case of TL (Mandowski, 2008).

The LM-OSL trap clustering effects shown in Fig. 4f are a new modeling result, not reported previously in the literature. These results show that trap clustering effects can occur for both TL and LM-OSL signals, and that they are more likely to occur in the case of small trap clusters with N_{traps}<200, and for conditions of strong retrapping.

4.3. The effect of retrapping in systems with small clusters

This section presents a systematic study of the effect of the retrapping ratio r on the trap clustering effects for TL and LM-OSL signals. Fig. 5 shows the variation of the number of remaining filled traps $n(T)$ as a function of temperature T, and for variable retrapping ratio r in the range r=1–10^3. Fig. 6 shows the corresponding TL signals. In this example there are two initially filled traps per cluster ($n_{filled}=N_{traps}=2$), and the total number of initially filled traps in the simulated system is $n_o=N_{clusters}n_{filled}=2\times10^5$.

At low values of the retrapping ratio $r = 1$ (circles in Fig. 5), the number of carriers $n(T)$ decreases continuously at all temperatures T, and the corresponding TL signal in Fig. 6a apparently consists of a single TL peak. However as the value of r is increased (r=10–10^3) in Fig. 5, it is clear that $n(T)$ follows a "two-step" variation, with the charge carriers recombining at progressively higher temperatures as r is increases. The corresponding TL intensities in Fig. 6b–d show clearly that the TL glow curve consists of 2 underlying peaks, which become more separated in temperature as r increases. This is consistent with previous simulations by Mandowski and Świątek (1998), who showed that the number of constituent TL peaks should be equal to the number of filled traps per cluster, in this case n_{filled}=2.

The physical picture behind the "two-step" variation of $n(T)$ in Fig. 5 can be interpreted as follows. Within each cluster of two initially filled traps, the retrapping term $A_n(N-n)$ is initially zero (since $n_{filled}=N_{traps}=2$), and hence there is initially a large probability of recombination and no retrapping takes place. Therefore one might expect about half of the electrons in the system (i.e. those corresponding to the first electron in each cluster) to recombine quickly at low temperatures, contributing to the first TL glow peak in Fig. 6 at a low temperature of ~120 °C. The recombination of the first electron within each cluster leads to a decrease of n, which leads to an increase of the retrapping term $A_n(N-n)$.

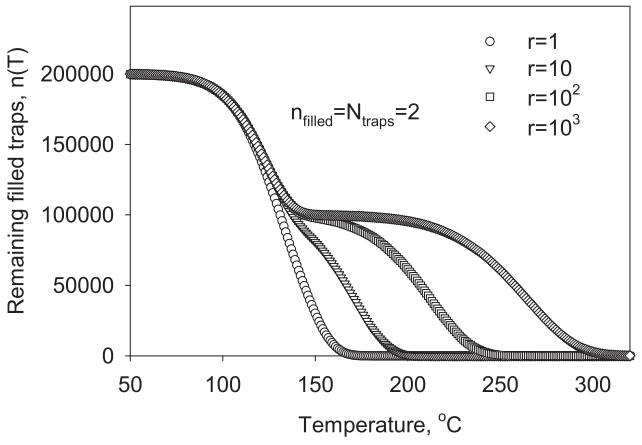

Fig. 5. Simulation of the effect of retrapping ratio $r=A_n/A_m$ on the variation of the remaining number of filled traps and for values of r=1–10^3. These simulations were carried out for small clusters with $n_{filled}=N_{traps}=2$. As the value of r increases, the charge carriers recombine at progressively higher temperatures. The number of remaining filled traps $n(T)$ follows a "two-step" variation explained in the text. The parameters are $s = 10^{10}$ s^{-1}, $E = 0.9$ eV, β=1 K/s.

Therefore the second electron within each trap cluster will have a much higher probability of being retrapped than the first electron, and therefore its recombination will occur at a higher temperature. The higher the retrapping ratio r, the higher the temperature at which the second TL glow peak appears. This succession of recombination events and increased retrapping probability will result in the second TL glow peak occurring at progressively higher temperatures as r increases, as shown in Figs. 5 and 6.

It is noted that the simulated two-peak TL glow curve shown in Fig. 6 are somewhat similar to the TL glow curves simulated within the much more complex kinetic model presented by Eliyahu et al. (2014) for LiF:Mg,Ti (TLD-100). This recent model considers both localized and delocalized transitions, leading to two simulated TL peaks corresponding to peaks 5 and 5a for this important dosimetric material.

Fig. 7 shows the same simulations as Fig. 6, for the case of LM-OSL signals and for the same parameters in the model. Fig. 7 shows clearly that the LM-OSL signals are also composites, with the number of constituent peaks in all cases being equal to n_{filled}=2. The higher the retrapping ratio r, the higher the stimulation time at which the second LM-OSL peak appears. However, as is well known from the theory of luminescence signals containing multiple components, there exists an important physical difference between the TL and LM-OSL signals shown in Figs. 6 and 7. As discussed for example in Kitis and Pagonis (2008), in LM-OSL signals all components start simultaneously at time $t = 0$, while in TL signals the various components appear in general sequentially at different temperatures, depending on the values of the kinetic parameters E,s for each component.

4.4. Large clusters-transition to the uniform distribution model

Fig. 8 shows the results of systematically increasing the size of clusters in the system, while keeping the total number of particles in the system fixed. Specifically TL glow curves are shown for several cases of small clusters ($n_{filled}=N_{traps}$=2,3,5,100). Fig. 9 shows the corresponding results for an LM-OSL signal, with similar conclusions.

In all cases shown in Fig. 8 the number of constituent TL peaks is equal to n_{filled}, and these results provide a demonstration of the transition from the small cluster behavior to the uniform distribution model of luminescence. In Fig. 8a–d, the low temperature TL peak appears at more or less the same temperature of ~120 °C. As the value of n_{filled} becomes large in Fig. 8d, this first TL peak becomes less prominent than the higher temperature composite TL peak appearing between 200 and 400 °C.

In Fig. 8ab and 9ab with $n_{filled}=N_{traps}$=2,3 there are clearly 2 and 3 constituent peaks in the TL and LM-OSL signals correspondingly. For systems with large clusters $n_{filled}\geq5$, all higher temperature constituent peaks of the TL and LM-OSL signals overlap strongly, and one obtains the continuous result for large clusters corresponding to the solution of the differential equations (shown as a solid line in Figs. 8d and 9d). The area of peak #1 in these simulated signals stays the same in all cases shown, while the area of peak #2 increases as the number of initially filled traps in the cluster (n_{filled}) increases. The total area in Figs. 8 and 9 is equal to the total number of initially filled traps $n_o=5\times10^4$.

These results are consistent with the physical interpretation of peak #1 corresponding to direct recombination (no retrapping), while peak #2 corresponds to electrons which have been retrapped perhaps several times before recombining at the luminescence centers. The conclusions from Fig. 9 for LM-OSL signals are very similar, with the important difference that all constituent signals start at once at time $t = 0$, as was discussed above.

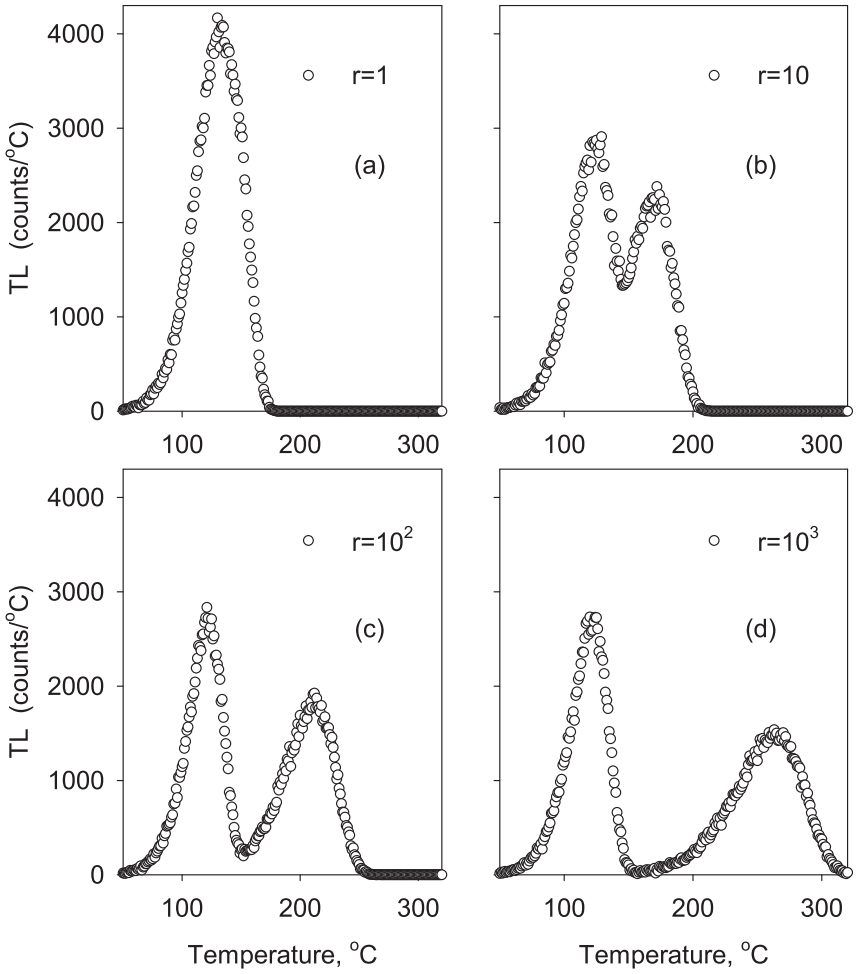

Fig. 6. The TL intensity $I_{TL}(T)$ calculated from the simulated curves of Fig. 5, indicating that the TL glow curve is a composite of 2 underlying peaks.

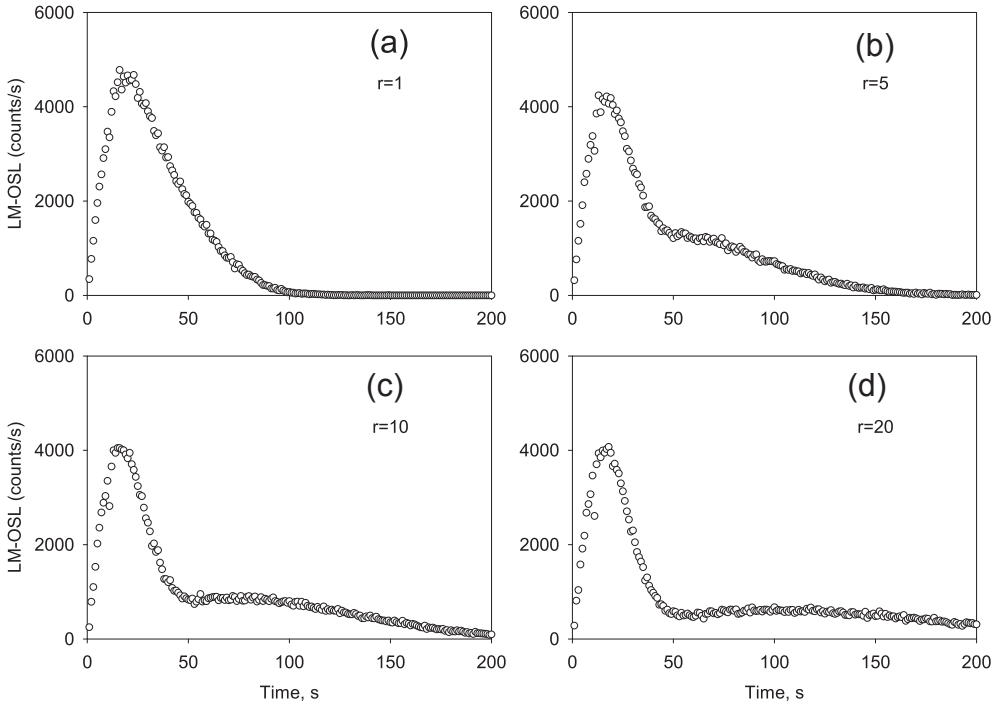

Fig. 7. Results of repeating the simulations in Fig. 6, for the case of LM-OSL signals. The model parameters are discussed in the text.

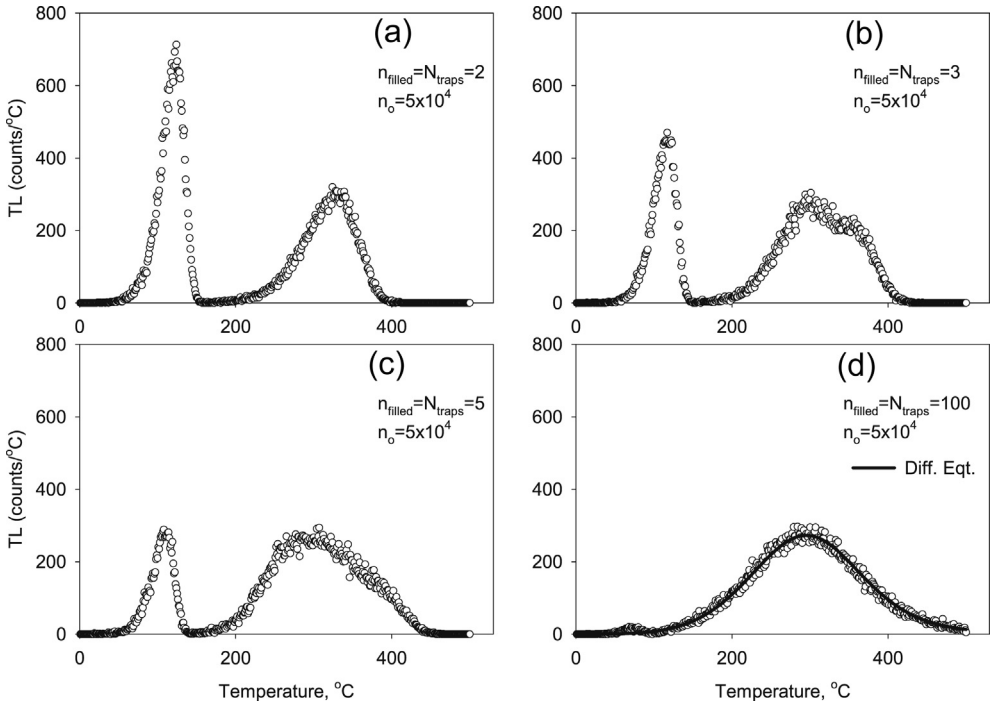

Fig. 8. Simulated TL glow curves for several cases of small clusters which are initially completely filled. The parameters are $n_{filled}=N_{traps}=2,3,5,100$ for cases (a) to (d). In all cases the total number of constituent TL peaks is equal to n_{filled}. In case (d) the TL glow curve approaches the solution of the differential equation, shown by the solid line. The parameters are $s = 10^{10}$ s^{-1}, $E = 0.9$ eV, $\beta = 1$ *K/s*, $r = A_n/A_m = 10^4$, $n_o=5\times10^4$.

5. Discussion

It is emphasized that the purpose of this paper is not to present a complete model of stochastic processes in luminescent materials, but rather to demonstrate that trap clustering effects can be derived mathematically as a stochastic process within the GOT model. As mentioned previously, the system simulated in this paper consists of many independent clusters of electron–hole pairs. Electrons are released from the traps and into the conduction band by either thermal or optical stimulation. Subsequently they are either recombined radiatively or are retrapped, with both retrapping and recombination taking place *within the same cluster.*

Due to these rather severe physical assumptions, the simple model presented in this paper is rather limited in its scope. In

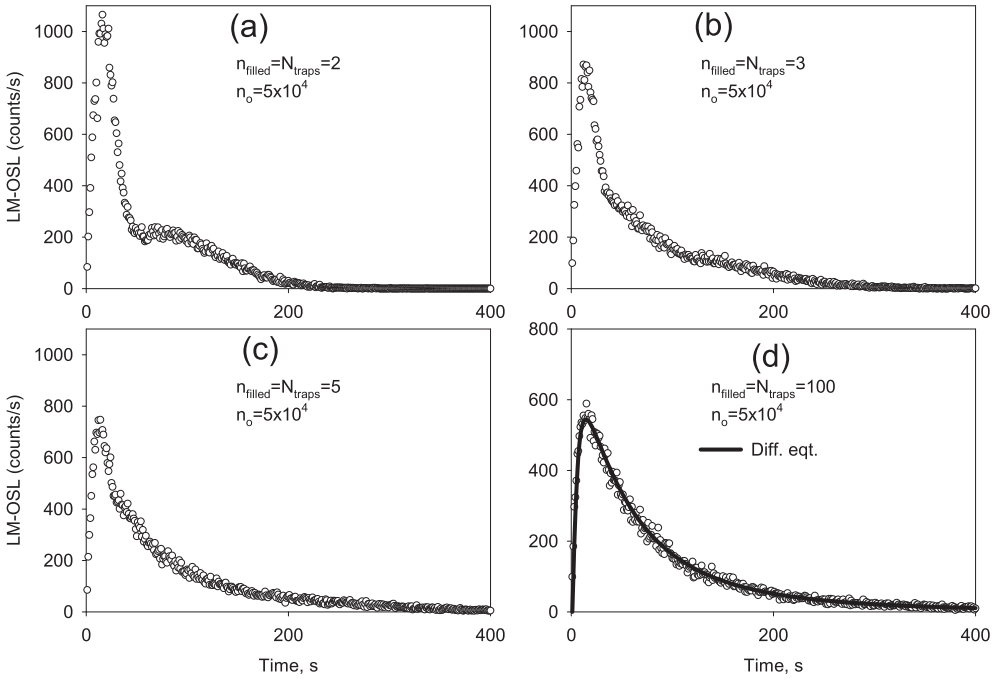

Fig. 9. Results of repeating the simulations in Fig. 8, for the case of LM-OSL signals. The parameters are $b = 0.002$ s^{-1}, $r = 10$, $n_o=5\times10^4$.

principle, one should consider a more comprehensive model which would also allow electrons to participate in both localized and delocalized transitions. For an example of such a comprehensive model, the readers are referred to the recent work by Eliyahu et al. (2014) for LiF:Mg,Ti (TLD-100).

Furthermore, the Monte Carlo method presented in this paper is restricted to systems in which the QE conditions are valid. This is in contrast to the Monte Carlo methods used by Kulkarni (1994) and by Mandowski (2008), which are more general and can be used whether the QE conditions hold or not. One would then expect that the simplified "brute force" Monte Carlo method in this paper will in general yield different results from these more complex methods which are based on transitions involving the conduction band. An additional important difference is that the results presented in this paper depend only on the retrapping ratio $r=A_n/A_m$ appearing in equations (12) and (13), and not on the actual numerical values of A_n and A_m. By contrast, the results from the models of Mandowski and Kulkarni (as well as the validity of the QE conditions) will depend on the actual numerical values of A_n,A_m and N. A direct comparison of results from the simplified and the full Monte Carlo methods is beyond the purpose of this paper, and will be the subject of an additional study presented elsewhere.

Even though the simplified method presented here will not be applicable for all luminescence systems, it is interesting to note that several of the general conclusions from this paper are very similar to the conclusions reached in the detailed studies by Mandowski (2008). In particular, both the simplified and the more complex Monte Carlo techniques predict the presence of multiple TL and LM-OSL peaks when one is dealing with small clusters and strong retrapping conditions.

Mandowski and Świątek (1996) showed that in the case of small clusters containing two traps per cluster and under conditions of high retrapping probability, the simulated glow curves consist of two closely situated peaks which can be described well by first order kinetics. These authors suggested that the activation energy values obtained from analysis of these two peaks have no physical meaning, and they recommended using care when analyzing TL glow curves resulting from a combination of localized and delocalized processes. In the physically similar example shown in Fig. 6d of this paper, it is found that peak #1 can be fitted with a first order TL peak described by the E,s values in the model. This is not surprising, since this first peak corresponds to direct recombination process with no retrapping. However, the higher temperature peak #2 in Fig. 6d obviously cannot be fitted with these same parameters due to strong retrapping effects.

The advantage of the method presented here is its simplicity and ease of use, and the fact that it can be easily generalized for other types of physical systems, as long as these systems can be described by a single differential equation similar to equation (12) in this paper. Specifically the method described in this paper was applied to a recently published model by Jain et al. (2012), which quantifies localized electronic recombination of donor–acceptor pairs in luminescent materials. Specifically the method was applied to the semi-analytical version of the model by Jain et al. (2012) presented by Kitis and Pagonis (2013), who showed that the system of simultaneous differential equations can be approximated to a very good precision by a single differential equation, in which the recombination probability varies with time during the stimulation process. When the presence of small clusters is assumed in this model and conditions of high retrapping prevail, the Monte Carlo method in this paper leads to strong trap clustering effects for both TL and infrared stimulated luminescence signals (IRSL) in this model. These results will be presented elsewhere.

References

Adamiec, G., Garcia-Talavera, M., Bailey, R.M., Iniguez de la Torre, P., 2004. Application of a genetic algorithm to finding parameter values for numerical stimulation of quartz luminescence. Geochronometria 23, 9–14.

Adamiec, G., Bluszcz, A., Bailey, R., Garcia-Talavera, M., 2006. Finding model parameters: genetic algorithms and the numerical modelling of quartz luminescence. Radiat. Meas. 41, 897–902.

Bailey, R.M., 2004. Paper I: simulation of dose absorption in quartz over geological timescales and its implications for the precision and accuracy of optical. Radiat. Meas. 38, 299–310.

Chen, R., Pagonis, V., 2011. Thermally and Optically Stimulated Luminescence: a Simulation Approach. Wiley and Sons, Chichester.

Chen, R., Pagonis, V., 2013. On the quasi-equilibrium assumptions in the theory of thermoluminescence(TL). J. Lumin. 143, 734–740.

Eliyahu, I., Horowitz, Y.S., Oster, L., Druzhyna, S., Mardor, I., 2014. Nanodosimetric kinetic model incorporating localized and delocalized recombination: application to the prediction of the electron dose response of the peak 5a/5 ratio in the glow curve of LiF: Mg,Ti (TLD-100). Radiat. Meas., 1–6. http://dx.doi.org/10.1016/j.radmeas.2014.01.015.

Gould, H., Tobochnik, J., 1995. An Introduction to Computer Simulation Methods. Applications to Physical Systems, 3 ed. Addison-Wesley.

Jain, M., Guralnik, B., Andersen, M.T., 2012. Stimulated luminescence emission from localized recombination in randomly distributed defects. J. Phys. Condens. Matter 24, 385402 (12pp).

Kitis, G., Pagonis, V., 2008. Computerized curve deconvolution analysis for LM-OSL. Radiat. Meas. 43, 737–741.

Kitis, G., Pagonis, V., 2013. Analytical solutions for stimulated luminescence emission from tunneling processes in random distributions of defects. J. Lum. 137, 109–115.

Kulkarni, R.N., 1994. The development of the Monte Carlo method for the calculation of the thermoluminescence intensity and the thermally stimulated luminescence. Radiat. Prot. Dosim. 51, 95–105.

Landau, D.P., Binder, K., 2013. A Guide to Monte Carlo Simulations in Statistical Physics, third ed. Cambridge University Press.

Mandowski, A., Świątek, J., 1992. Monte Carlo simulation of thermally stimulated relaxation kinetics of carrier trapping in microcrystalline and two-dimensional solids. Phil. Mag. B 65, 729–732.

Mandowski, A., Świątek, J., 1996. On the influence of spatial correlation on the kinetic order of TL. Radiat. Prot. Dosim. 65, 25–28.

Mandowski, A., Świątek, J., 1998. Thermoluminescence and trap assemblies—results of Monte Carlo calculations. Radiat. Meas. 29, 415–419.

Mandowski, A., Świątek, J., 2000. The kinetics of trapping and recombination in low dimensional structures. Synth. Met. 109, 203–206.

Mandowski, A., 2001. Modelling of charge carriers' transport and trapping phenomena in one-dimensional structures during thermal stimulation. J. Electr. 51–51, 585–589.

Mandowski, A., 2006. Calculation and properties of trap structural functions for various spatially correlated systems. Radiat. Prot. Dosim. 119, 85–88.

Mandowski, A., 2008. How to detect trap cluster systems? Radiat. Meas. 43, 167–170.

Mandowski, A., Bos, A.J.J., Mandowska, E., Orzechowski, J., 2010. Monte-Carlo method for determining the quenching function from variable heating rate measurements. Radiat. Meas. 45, 284–287.

Pagonis, V., Kitis, G., Furetta, C., 2006. Numerical and Practical Exercises in Thermoluminescence. Springer, p. 51.

Pagonis, V., Kitis, G., 2012. Prevalence of first-order kinetics in thermoluminescence materials: an explanation based on multiple competition processes. Phys. Status Solidi B 249, 1590–1601.

Pagonis, V., Chen, R., Kitis, G., 2011. On the intrinsic accuracy and precision of luminescence dating techniques for fired ceramics. J. Archaeol. Sci. 38, 1591–1602.

Rodríguez-Villafuerte, M., 1999. A Monte Carlo approach to the track interaction model to explain supralinearity in the thermoluminescence response. Nucl. Inst. Meth. Phys. Res. B 152, 105–114.

Salah, N., 2011. Nanocrystalline materials for the dosimetry of heavy charged particles: a review. Radiat. Phys. Chem. 80, 1–10.

Sun, H.T., Sakka, Y., 2014. Luminescent metal nanoclusters: controlled synthesis and functional applications. Sci. Technol. Adv. Mater. 15, 014205. http://dx.doi.org/10.1088/1468–6996/15/1/014205.

Thompson, J.W., 2007. Accuracy, precision, and irradiation time for Monte-Carlo simulations of single aliquot regeneration (SAR) optically stimulated luminescence (OSL) dosimetry measurements. Radiat. Meas. 42, 1637–1646.